Magnetic Properties and Electronic Structure of CeTIn (T = Ni, Cu, Pd, Au) Compounds

A. Szytuła, B. Penc

M. Smoluchowski Institute of Physics, Jagiellonian University
Reymonta 4, 30-059 Kraków, Poland

and Ł. Gondek

Faculty of Physics and Applied Computer Science
AGH University of Science and Technology
al. Mickiewicza 30, 30-059 Kraków, Poland

Dedicated to Professor Józef Spałek on the occasion of his 60th birthday

The electronic structure of the ternary CeTIn (T = Ni, Cu, Pd, Au) compounds was investigated by means of X-ray photoelectron spectroscopy. Our interest was aimed mainly to the valence bands and the Ce3d core levels of investigated compounds. Analysis of the valence bands indicates that they are mainly determined by the Tnd band, whereas a share of the R4f states can be estimated to be about a few percent only. The analysis of the differential valence bands spectra between CeTIn and LaTIn analogues suggests that the Ce4f^1 ground states shift deeper below the Fermi level with an increase in the 4f level occupation factor. The analysis of the Ce3d spectra made on the basis of the Gunnarsson–Schönhammer model indicates the hybridization parameter equal to 148 meV for CeNiIn, 45 meV for CeCuIn, 177 meV for CePdIn, and 123 meV for CeAuIn.

PACS numbers: 71.20.Eh, 71.27.+a, 75.20.Hr, 79.60.–i

1. Introduction

A broad spectrum of unusual physical properties of the cerium-based compounds originates mainly from the hybridization of the Ce4f electrons with the conduction band or/and with the d or p states of ligands atoms. It results with a great variety of interesting features as intermediate valence, Kondo behaviour,

spin fluctuations, heavy fermions, and quantum critical phenomena. The properties of strongly correlated $4f$ electron systems can be explained basing on some information about the nature of Ce$4f$ ground state. Within this paper we report systematic studies of intermetallic Ce-based indides.

Ternary Ce–T–X compounds, where T is d-electron element and X is p-electron element, crystallize in a few different stoichiometries. The compounds of 1:2:2 stoichiometry have been a subject of extensive studies [1], consequently the data concerning these phases reaches about 50% of the all data related to cerium--based compounds. Among 1:2:2 compounds the CeCu$_2$Si$_2$ is especially interesting. The compound exhibits superconductivity below 0.5 K, moreover an extremely large value of the electronic specific heat $\gamma = 1.1$ J/(mol K^2) suggests that CeCu$_2$Si$_2$ is a heavy fermion system with an effective electron mass of approximately $100m_e$ [2].

Intermetallic CeTX compounds form an interesting group as well. A short overview on the unusual low temperature properties of CeTX compounds was given by Adroja and Malik [3] and Fujita et al. [4]. These compounds crystallize in different types of the crystal structure. Most of these compounds exhibit hexagonal or orthorhombic crystal structures.

The magnetic studies of 1:1:1 compounds indicate that the majority of them order antiferromagnetically at low temperatures. This is supported by observation of the negative value of the paramagnetic Curie temperature in these compounds. The values of the effective magnetic moments determined from the magnetic susceptibility in the paramagnetic region are close to the free Ce^{3+} ion value ($2.54\mu_B$). On the other hand, the values of the cerium magnetic moments in the magnetically ordered state ranging from $0.64\mu_B$ for CePtSb [5] up to $1.66\mu_B$ for CeCuGe [6] and are lower than the value for free Ce^{3+} ion ($2.54\mu_B$). The observed decreases in the values of the Ce magnetic moments are probably due to hybridization between Ce$4f$ electrons (responsible for the localized magnetic moments) and the conduction band or/and d and p states of the T- and X-element, respectively.

The CeTIn compounds crystallize in the hexagonal ZrNiAl-type crystal structure [7, 8]. Within the crystal unit cell atoms occupy the following positions: Ce atoms 3(f) site: x_{Ce}, 0, 0; T atoms 1(a) site: 0, 0, 0 and 2(d) site: 1/3, 2/3, 1/2 and In atoms 3(g) site: x_{In}, 0, 1/2. The ZrNiAl-type structure rises a topological frustration of the Ce$4f$ moments originating from the triangular coordination of Ce atoms. For all these compounds some correlation between magnetic properties and unit cell volume is observed. With an increase in the unit cell volume magnetic properties change from the Pauli paramagnet for CeNiIn to antiferromagnetically ordered CePdIn ($T_N = 1.8$ K) and CeAuIn ($T_N = 5.7$ K). Simultaneously, a decrease in the Kondo temperature from $T_K = 94$ K for CeNiIn [9] to 3.3 K for CePdIn [10] was reported. In contrast to the antiferromagnetically ordered CePdIn, no signs of magnetic ordering were evidenced for heavy-fermion and dense-Kondo CePtIn compound down to 50 mK [11]. CeRhIn was reported

to be a mixed-valence system [12]. Electronic properties of the $CePd_xRh_{1-x}In$ ($0 \leq x \leq 1$) solid solution were reported by Brück et al. [13]. Magnetic properties are continuously changing with x from unstable $4f$ moments for CeRhIn to localized $4f$ moments in CePdIn. The electronic specific heat coefficient γ increases from 40 mJ/(mol K^2) for $x = 0$ by 78 mJ/(mol K^2) ($x = 0.2$), 280 mJ/(mol K^2) ($x = 0.4$), 700 mJ/(mol K^2) ($x = 0.6$) to 123 mJ/(mol K^2) for $x = 1.0$. Similarly to CeNiIn compound, CeCuIn one remains paramagnetic down to 1.7 K [14].

The photoemission spectroscopy (PES) is considered to be the most successful way to study the nature of the Ce$4f$ states [15]. The main aim of our investigations was to find correlations between crystal structure, electronic structure, and magnetic properties of investigated compounds. In principle, information about hybridization of the $4f$ levels in Ce should be accessible from direct measurements of the $4f$ level in photoemission spectra of the valence band (VB). In practice, the small cross-section of $4f$ states comparing to the d ones makes any analyses very hard when using classical photoemission. More reliable information about the $4f$ states can be achieved using resonant photoemission. Also the Ce$3d$ core-level photoemission lines have been widely used to diagnose hybridization strength of the $4f$ levels in Ce-based systems [15].

In this work, we present the data concerning the electronic structure of CeTIn (T = Ni, Cu, Pd, Au) compounds and its correlation with magnetic properties of these compounds. The influence of the hybridization is discussed as well.

2. Experimental details

Polycrystalline samples of CeTIn (T = Ni, Cu, Pd, Au) compounds were obtained by arc melting of stoichiometric amounts of the elements (Merck AG: Ce of 99.9% purity, Ni, Cu, Pd, Au, and In of 99.99% purity) under a high-purity argon atmosphere on a water-cooled copper hearth, using a titanium-zirconium alloy as a getter. In order to ensure good homogeneity the buttons were turned over and remelted several times. The final weight losses were lower than 0.1%. Subsequently the samples were annealed in evacuated quartz tubes at 800°C for one week. The quality of the products was checked by X-ray powder diffraction using Philips PE-3710 apparatus (Cu K_α radiation) at the room temperature. All of the reflections were indexed within the hexagonal structure of ZrNiAl-type. For processing the collected data Rietveld-type program Fullprof was used [16]. The determined structural parameters for CeTIn compounds are collected in Table I.

The X-ray photoelectron spectra (XPS) were obtained at room temperature using the SPECS LHS 10+ photoelectron spectrometer with the Mg K_α ($h\nu = 1253.6$ eV) and Al K_α ($h\nu = 1486.6$ eV) radiation sources. The overall resolution is 0.75 eV. Binding energies were referred to the Fermi level ($E_F = 0$). The spectrometer was calibrated using the Cu$2p_{3/2}$ (932.5 eV), Ag$3d_{5/2}$ (368.1 eV) and Au$4f_{7/2}$ (84.0 eV) core-level photoemission spectra. Surfaces of the samples were mechanically cleaned by scraping with a diamond file in a preparation chamber

TABLE I

Parameters of the crystal structure of CeTIn (T = Ni, Cu, Pd, Au) compounds.

T	a [Å]	c [Å]	c/a	z_{Ce}	z_{In}
Ni	7.520(1)	3.9734(8)	0.528	0.590(2)	0.254(2)
Cu	7.942(2)	4.2452(15)	0.5667	0.592(1)	0.240(1)
Pd	7.7003(4)	4.0741(3)	0.529	0.583(1)	0.248(1)
Au	7.688(1)	4.262(1)	0.554	0.592(1)	0.241(2)

under high vacuum conditions (10^{-9} mbar), then the samples were immediately moved into the analysis chamber. This procedure was repeated until the C1s and O1s surface impurities core-level peaks were negligibly small. The Shirley method was used to subtract background, the experimental spectra prepared in this manner were numerically fitted using the 80% Gaussian and 20% Lorentzian peak-shape [17].

3. Electronic structure of CeTIn compounds

Figure 1 shows the XPS spectrum of CeCuIn collected in a wide 0–1000 eV binding energy range. The binding energies are related to the Fermi level ($E_F = 0$ eV). In general, the most important data are obtained from three regions: VB (binding energy 0–10 eV), Ce4d states (100–120 eV) and Ce3d (880–930 eV).
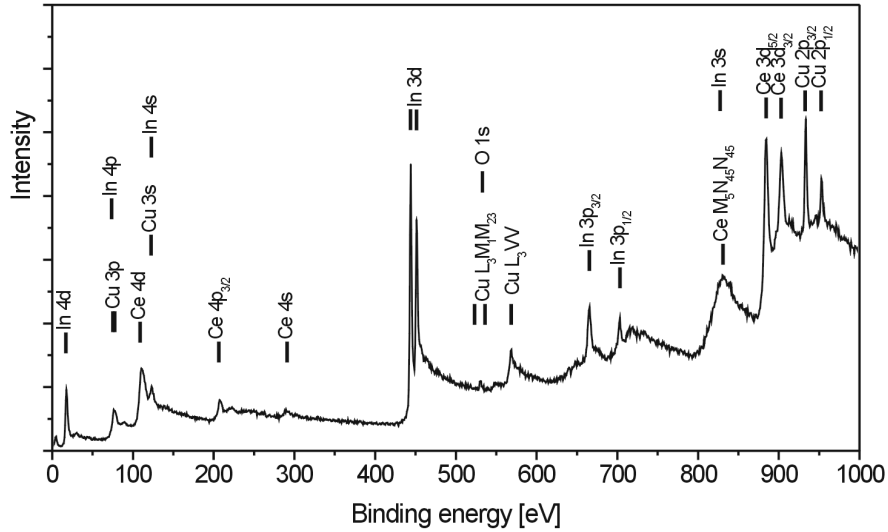

Fig. 1. Photoemission spectra of CeCuIn taken at the room temperature within 0–1000 eV binding energy range (Al K_α radiation).
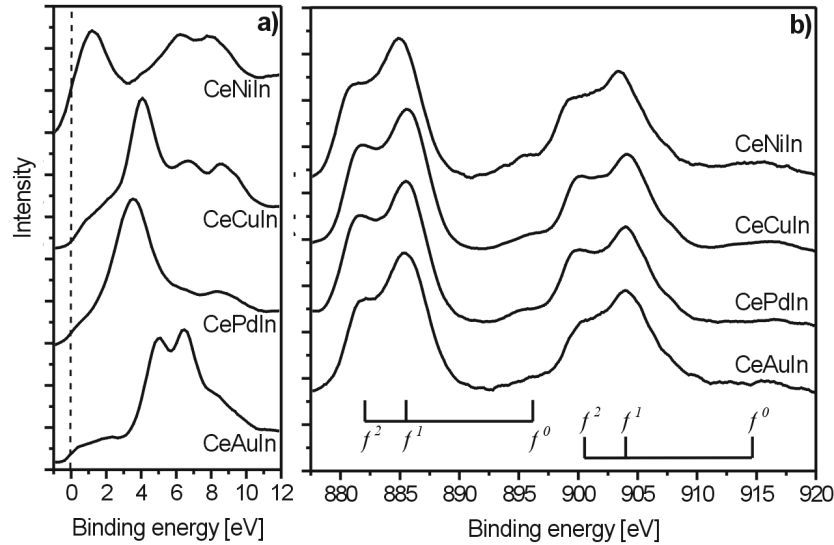
Fig. 2. Details of photoemission valence bands (a) and Ce3d core levels (b) spectra of CeTIn compounds. At the right part the positions of features originating from Ce4f electronic configuration are marked.

The XPS VB of all CeTIn compounds are presented in Fig. 2a. The band extends from the Fermi energy located at $E = 0$ eV to the binding energy of about 7.5 eV. The VB spectra represent mainly the dominant contribution of the Tnd states. The peaks corresponding to these states are at 1.2 eV for T = Ni, 4.0 eV for T = Cu and 3.5 eV for T = Pd, 5.0 and 6.5 eV for T = Au. Positions of these peaks are in good agreement with the calculated values [18]. For compounds with T = Cu, Pd and Au the nd states are deeper below the Fermi level (FL), thus just below the FL superposition of the Ce4f states and (5d6s) conduction band are visible.

At about 110 eV the broad peak of Ce4d states can be noticed. Unfortunately, in all investigated compounds a structure of this peak is disturbed by In4s states, making a deeper analysis impossible.

Information about 4f hybridization may be derived from the analysis of Ce3d core-level doublet (see Fig. 2b). For strongly hybridized systems, a splitting of the each Ce3d component into three components arising essentially from the $3d^9 4f^0$, $3d^9 4f^1$, and $3d^9 4f^2$ states is expected [15].

The analysis of these components was based on the Doniach–Šunjić theory [19]. Within this approach an intensity ratio $r_1 = I(f^2)/[I(f^2) + I(f^1)]$ can be calculated ($I(f^n)$ is the integral intensity of relevant component as marked in Fig. 2b). There is a relation between intensity ratio r_1 and Gunnarsson–Schönhammer parameter [15]. This relation enables calculation of the coupling parameter basing on the experimental Ce3d spectra deconvolution. The parame-

ter is defined as $\pi V_{cf}^2 \rho_{max}$, where ρ_{max} is the maximum of the density of conduction states and V_{cf} is the hybridization matrix element. On the other hand, the intensity ratio $r_2 = I(f^0)/[I(f^0) + I(f^1) + I(f^2)]$ provides an estimation of the occupation of the Ce4f shell. This relation is given as: $n^{XPS} = 1 - r_2$ [15]. The appearance of the f^0 contribution is a clear evidence of a mixed valence state. In our samples such anomaly can be noticed in the case of CeNiIn sample, consequently the occupation of the Ce4f shell is relatively low. All values calculated basing on Ce3d spectra (Δ and n^{XPS}) for investigated CeTIn compounds are listed in Table II. In Table II the available data for other CeTX compounds are summarized as well.

TABLE II

Volume per formula unit — V_{fu}; occupation of the final states from XPS — n_f; the hybridization parameter — Δ; magnetic behaviour — MB: PP — Pauli paramagnet, F — ferro, AF — antiferro, CWP — Curie–Weiss paramagnet, VF — valence fluctuation, MV — mixed valence, SF — spin fluctuation; $T_{C,N}$ — Curie or Néel temperature; T_K — Kondo temperature; γ — electronic coefficient of the specific heat in CeTX compounds.

Compound	V_{fu} [Å^3]	n_f	Δ [meV]	MB	$T_{C,N}$ [K]	T_K [K]	γ $\left[\frac{mJ}{mol\ K^2}\right]$	Ref.
CeNiAl	56.5	< 1	140	PP			12	[28]
CeCuAl	62.40	≈ 1	45	F	5.0			[28]
CeNiSn	65.12	∼ 1		PP(VF)		100	173	[29]
CePdSn	70.82	0.95		AF	7.5		60	[30]
CePtSn	69.22	∼ 1		AF	7.5	10	6.4	[31]
CeAgSn	76.50	∼ 1	165	AF	3.6			[32]
CeRhSn	68.32	1	120	*			75	[33]
CeNiIn	65.62	0.93	148	SF		94	60	this work, [4]
CeCuIn	71.53	0.84	45	CWP			40	this work
CeRhIn	66.81	0.92	100	MV*				[34]
CePdIn	70.0		170	AF	1.7	3.3	> 100	this work, [4]
CePtIn	68.8	0.97		CWP		11	700	[4]
CeAuIn	72.8		123	AF	5.7		30	this work, [35]
CeNiSb	68.98	0.91	∼ 50	F	4.6	15		[36]
CePdSb	72.17		∼ 50	F	17	15		[25]
CeRhSb	67.0	0.86	140	MV		360		[30]

*$\chi^{-1}(T)$ does not follow the Curie–Weiss law.

Within the frames of Harrison–Straub (HS) model a hybridization between rare earth 4f and transition metal d states can be estimated [20, 21]. This theory enables calculation of hybridization matrix element V_{df} as a function of interatomic distances as well as respective shell mean radii

$$V_{\mathrm{df}} = \frac{\eta_{ll'm}\hbar^2}{m_{\mathrm{e}}} \frac{\sqrt{r_l^{2l-1} r_{l'}^{2l'-1}}}{d^{l+l'+1}}, \tag{1}$$

where m_{e} — electron mass, r — mean radius of considered shell, d — interatomic distance, l — angular momentum quantum number, m — symmetry of bond ($m = 0$ for σ; $m = 1$ for π, $m = 2$ for δ; and $m = 3$ for ϕ). Parameter $\eta_{ll'm}$ is a complex function of angular momentum quantum numbers as well as symmetries of bonds [22]:

$$\eta_{ll'm} = \frac{(-1)^{l'+1}(-1)^m}{6\pi} \frac{(l+l')!(2l)!(2l')!}{2^{l+l'}l!l'!}$$

$$\times \sqrt{\frac{(2l+1)(2l'+1)}{(l+m)!(l-m)!(l'+m)!(l'-m)!}}. \tag{2}$$

When taking into account $f-d$ hybridization and $m = 0$ only, it is possible to derive V_{df} parameters for investigated compounds. This approach is not strictly quantitive, however a general trend for isostructural compounds can be deduced. The appropriate radii of considered shells were taken after Ref. [20]. The interatomic distances were calculated according to the X-ray diffraction data at the room temperature. The results are collected in Table III.

TABLE III

Harrison–Straub model parameters (d_{4f-nd} — Ce–T shortest distance, r_{nd} — nd shell radius, r_{4f} — Ce4f shell radius) and energetic separation between Ce4f states and Tnd ones for CeTIn compounds.

T	d_{4f-nd} [Å]	r_{nd} [Å]	r_{4f} [Å]	V_{df} [meV]	$\delta(E_{4f} - E_{nd})$ [eV]
Ni	3.019	0.601	0.445	88	0.7
Cu	3.208	0.657	0.445	70	2.0
Pd	3.082	0.980	0.445	162	1.3
Au	3.137	0.931	0.445	135	2.4

Within this approach a variation of energetic separation between hybridizing levels is not taken into account. In order to make some deeper conclusions an energetic separation between hybridizing levels should be considered as well. In order to estimate roughly the Ce4f contribution to the VB, a difference between appropriate CeTIn and LaTIn (empty 4f shell) compounds was taken. All spectra were normalized with respect to the In4d doublet, the background was extracted as well. All spectra were collected under the same conditions: step, time, pressure, pass energy, etc. The results are presented in Fig. 3. The maximum of the Ce4f contribution is located at 1.9 eV for T = Ni; 2.0 eV for T = Cu; 2.2 eV for T = Pd; and 2.6 eV for T = Au. According to resonant photoemission data reported for other intermetallic cerium-based compounds this maximum at about
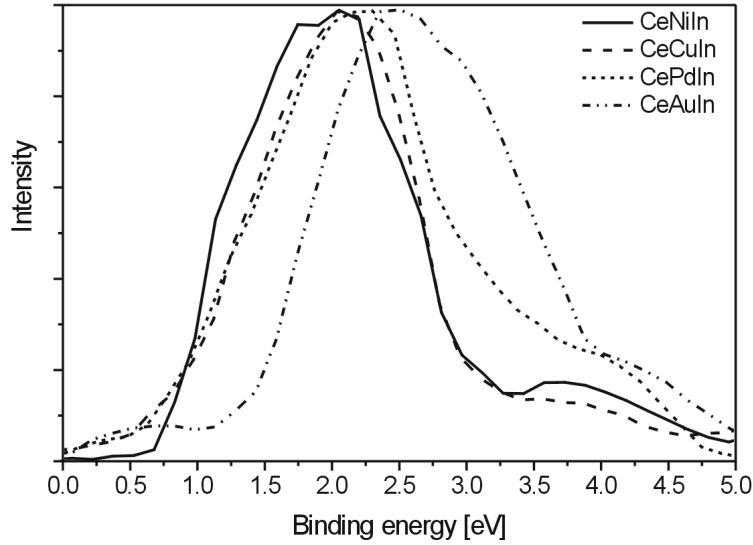
Fig. 3. Estimated Ce$4f$ contribution to the valence band spectra of CeTIn compounds.

≈ 2 eV can be attributed to f^0 final states [23]. The f^0 final states originate mainly due to photoemission of an electron from f^1 initial states. These initial states are responsible for Ce^{3+} configuration, which may exhibit magnetic ordering.

Now, it is possible to estimate the energetic separation between Ce$4f$ states and Tnd ones for all investigated compounds. Such comparison is given in Table III.

4. Discussion

The results of the XPS data presented in this work indicate:

- The existence of the mixed valence state in majority of these compounds. This result is in good agreement with the X-ray absorption data which for CeAuIn give the valence of cerium 3.03 [24]. As well, this is in good correlation with the macroscopic data (temperature dependence of the magnetic susceptibility, electrical resistivity).

- The Δ parameter is small (near 50 meV) for CeCuIn, CeCuAl, CeNiSb, and CePdSb or higher above 100 meV for the others. It is difficult to discover the apparent correlation between this parameter and other physical properties, however one may find intriguing that for low values of Δ only ferromagnetic behaviour is observed,

- Essential factors which determine the magnetic properties are $f-d$ hybridization and relative position of Ce$4f$ states (≈ 2 eV below the Fermi level) with respect to the Tnd states.

    The energetic separation between Ce4f and Tnd states as well as hybridization strength seems to be crucial for establishing magnetic ordering in cerium-based compounds. For compounds such as CeNiIn or CeRhIn this effect is large, consequently no localized magnetic moment on Ce atoms was observed. Moreover, for CeNiIn a high Kondo temperature ($\approx$ 94 K) was reported [9]. On the other hand, this effect is much lower in CeNiSb (the Δ does not exceed 50 meV and Kondo temperature is about 15 K). Consequently, this compound orders ferromagnetically [25].
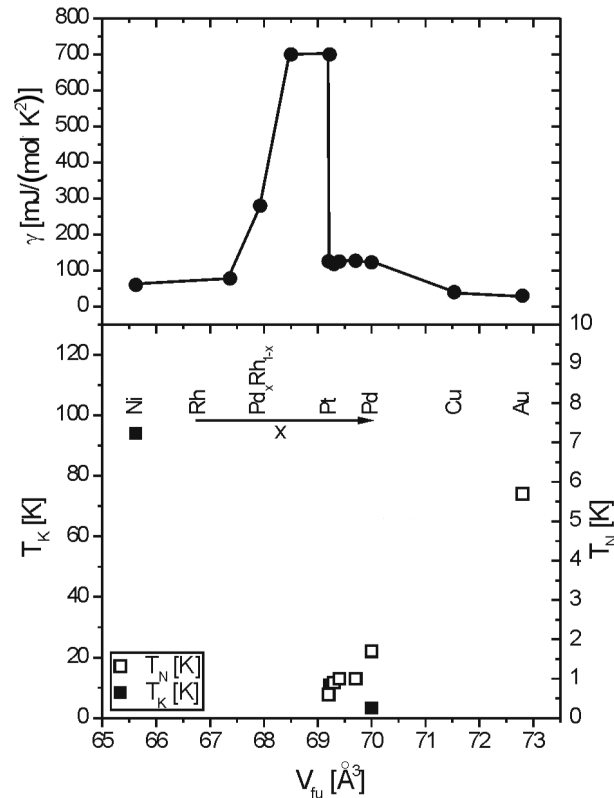

Fig. 4. Electronic specific heat γ coefficient and characteristic temperatures (T_{K} — Kondo temperature, T_{N} — Néel temperature) versus volume per formula unit for CePd$_x$Rh$_{1-x}$In and other CeTIn compounds. The solid line in the upper part is given for an eye.

    Also the interatomic distances influence the magnetic properties of these compounds. According to Eq. (1) the hybridization matrix elements are lowering when the distances between hybridizing shells are rising. In Fig. 4 the Kondo and Néel temperatures, the electronic coefficient of the specific heat for CeTIn and CePd$_x$Rh$_{1-x}$In compounds, plotted as a function of the volumes per formula unit

are presented. The compounds with small unit cell volumes exhibit the Kondo behaviour and hence no long-range order is observed. Also CeNiIn and CeRhIn are valence fluctuation systems with no magnetic order. Paramagnetic CeCuIn compound lies in the intermediate region, similar to the CePtIn which is a heavy fermion paramagnet. CePdIn and CeAuIn are antiferromagnets while they exhibit large unit cell volumes.

In general, the higher unit cell volume becomes, the lower Kondo temperature and the higher ordering temperature are observed. This is an interesting observation that a sharp increase in the coefficient occurs in the region of a change from Kondo to magnetic ordering regime.

The above-mentioned properties can be qualitatively explained according to the Doniach phase diagram [26]. Within this model the Kondo temperature T_{K} exhibits exponential dependence on the exchange constant J_{cf} between the $4f$ and conduction electrons. On the other hand, characteristic temperature T_{RKKY} of the Ruderman–Kittel–Kasuya–Yoshida (RKKY) interaction is proportional to J_{cf}^2. Consequently, at lower J_{cf} values RKKY interactions are dominant. When J_{cf} rises, a crossover between RKKY magnetic metal and non-magnetic Kondo regime is observed. Such behaviour is observed in CePdIn compound, where both interactions are present (see Table II). The non-magnetic Kondo regime holds for high values of J_{cf} (eg. CeNiIn). In limit of large Coulomb repulsion U_{f-f}, J_{cf} is proportional to $V_{\mathrm{cf}}^2/(E_{\mathrm{F}} - E_{4f})$, where V_{cf} is the mixing parameter between the $4f$ and conduction electrons, E_{F} is the Fermi energy and E_{4f} stands for the $4f$ level energy.

A deeper discussion can be performed for CeTIn compounds when the transition metal elements are from the same column of the periodic table (T = Ni, Pd, Pt). In this series the density of states at the Fermi level $\rho(E_{\mathrm{F}})$ decreases because the Tnd states shift below the Fermi level. In these systems the nearest-neighbour distance $d_{\mathrm{Ce-T}}$ between the cerium and T atoms increases in the following manner: $d_{\mathrm{Ce-Ni}}(\mathrm{CeNiIn}) < d_{\mathrm{Ce-Pt}}(\mathrm{CePtIn}) < d_{\mathrm{Ce-Pd}}(\mathrm{CePdIn})$. This suggests that the values of $J_{\mathrm{cf}}(\mathrm{CeNiIn}) > J_{\mathrm{cf}}(\mathrm{CePtIn}) > J_{\mathrm{cf}}(\mathrm{CePdIn})$ which is in agreement with the proposed Doniach diagram for these compounds [3].

The influence of the hybridization of Ce$4f$ electrons with nd electrons of the T element is also observed in binary cerium compounds. For example CePd is ferromagnet with $T_{\mathrm{C}} = 6.5$ K, whereas CeNi and CeRh are mixed valence system [27].

Recently it has been shown that hydrogenating of ternary compounds (e.g. CePdIn, CeNiIn) leads to suppressing the Kondo interaction due to expansion of the crystal unit cell volume [37, 38]. The CeNiInH$_{1.8}$ compound exhibits magnetic ordering with $T_{\mathrm{C}} = 6.8$ K [37]. Hydrogenating of magnetic Kondo compounds (e.g. CePdIn) leads to an increase in the ordering temperature, thus one may conclude that the Kondo interaction are lowered as in the case of CeNiIn as well [37]. A similar behaviour was reported in the case of hydrogenated CeRhIn compound,

where the expansion of the unit cell turns the compound from mixed valence into stable trivalent regime [39]. The above observations are in agreement with the Harrison–Straub model (see Eq. (1)) where the hybridization matrix elements vanish strongly with a rise of the interatomic distances.

Acknowledgments

References

[1] A. Szytuła, J. Leciejewicz, *Handbook of Crystal Structures and Magnetic Properties of Rare Earth Intermetallics*, CRC Press, Boca Raton 1994.

[2] G.R. Stewart, *Rev. Mod. Phys.* **56**, 755 (1984).

[3] D.T. Adroja, S.K. Malik, *J. Magn. Magn. Mater.* **100**, 126 (1991).

[4] T. Fujita, T. Suzuki, S. Nishigori, T. Takabatake, H. Fujii, J. Sakurai, *J. Magn. Magn. Mater.* **108**, 35 (1992).

[5] B.D. Rainford, D.T. Adroja, *Physica B* **194-196**, 365 (1994).

[6] H. Nakotte, Ph.D. Thesis, University of Amsterdam, Amsterdam 1994.

[7] Ya.M. Kalychak, *Izv. Akad. Nauk USSR, Metally* **4**, 110 (1998) (in Russian).

[8] P. Villars, L.D. Calvert, *Pearson's Handbook of Crystallographic Data for Intermetallic Phases*, 2nd ed., ASM International, Materials Park (Ohio) 1991.

[9] H. Fujii, T. Inoue, Y. Andoh, T. Takabatake, K. Satoh, Y. Maeno, T. Fujita, J. Sakurai, Y. Yamaguchi, *Phys. Rev. B* **39**, 6840 (1989).

[10] H. Fujii, M. Nagasawa, H. Kawanaka, T. Inoue, T. Takabatake, *Physica B* **165**, 435 (1990).

[11] T. Fujita, K. Satoh, Y. Maeno, Y. Uwatoko, H. Fujii, *J. Magn. Magn. Mater.* **76-77**, 133 (1988).

[12] D.T. Adroja, S.K. Malik, B.D. Padalia, R. Vijayaraghavan, *Phys. Rev. B* **39**, 4831 (1989).

[13] E. Brück, H. Nakotte, K. Bakker, F.R. de Boer, P.F. de Châtel, J.-Y. Li, J.P. Kuang, F.M. Yang, *J. Alloys Comp.* **200**, 79 (1993).

[14] A. Szytuła, D. Kaczorowski, M. Kalychak, B. Penc, Yu. Tyvanchuk, *J. Alloys Comp.*, in press.

[15] J.C. Fuggle, F.U. Hillebrecht, Z. Żołnierek, R. Lasses, Ch. Frieburg, O. Gunnarsson, K. Schönhammer, *Phys. Rev. B* **27**, 7330 (1983).

[16] J. Rodriguez-Carvajal, *Physica B* **192**, 55 (1993).

[17] D.A. Shirley, *Phys. Rev. B* **5**, 4709 (1975).

[18] Ł. Gondek, B. Penc, A. Szytuła, A. Jezierski, A. Zygmunt, *Acta Phys. Pol. B* **34**, 1209 (2003).

[19] S. Doniach, M. Šunjić, *J. Phys. C* **3**, 285 (1970).

[20] G.K. Straub, W.A. Harrison, *Phys. Rev. B* **31**, 7668 (1985).

[21] W.A. Harrison, G.K. Straub, *Phys. Rev. B* **36**, 2695 (1987).

[22] J.M. Willis, W.A. Harrison, *Phys. Rev. B* **28**, 4363 (1983).

[23] A. Sekiyama, T. Iwasaki, K. Matsuda, Y. Saitoh, Y. Ônuki, S. Suga, *Nature* **403**, 396 (2000).

[24] D. Wohlleben, J. Rohler, *J. Appl. Phys.* **55**, 1904 (1984).

[25] S.K. Malik, D.T. Adroja, *Phys. Rev. B* **43**, 6295 (1991).

[26] S. Doniach, *Physica B* **91**, 231 (1977).

[27] J.G. Sereni, in: *Handbook on the Physics and Chemistry of Rare Earths*, Vol. 15, Eds. K.A. Gschneidner, Jr., L. Eyring, North-Holland, Amsterdam 1991, Ch. 98, p. 1.

[28] R.K. Singha, N.L. Saini, K.B. Garg, J. Kanshi, L. Ilver, P.O. Milsson, Ravi Kumar, L.C. Gupta, *J. Phys., Condens. Matter* **5**, 4013 (1993).

[29] A. Ślebarski, A. Jezierski, *Mol. Phys. Rep.* **38**, 47 (2003).

[30] D.T. Adroja, S.K. Malik, *Phys. Rev. B* **45**, 779 (1992).

[31] H. Kadowaki, T. Ekimo, H. Iwasaki, T. Takabotake, H. Fujii, J. Sakurai, *J. Phys. Soc. Jpn.* **62**, 4426 (1993).

[32] D. Fus, V. Ivanov, A. Jezierski, B. Penc, A. Szytuła, *Acta Phys. Pol. A* **98**, 571 (2000).

[33] A. Ślebarski, M.B. Maple, E.J. Freeman, C. Sirvent, M. Radłowska, A. Jezierski, E. Grando, Q. Huang, J.W. Lynn, *Philos. Mag. B* **82**, 943 (2002).

[34] A. Ślebarski, private communication.

[35] H.R. Pleger, E. Brück, E. Braun, F. Oster, A. Freimuth, B. Politt, B. Roden, D. Wohlleben, *J. Magn. Magn. Mater.* **63-64**, 107 (1987).

[36] Latika Menon, S.K. Malik, *Phys. Rev. B* **52**, 35 (1995).

[37] B. Chevalier, A. Wattiaux, J.-L. Bobet, *J. Phys., Condens. Matter* **18**, 1743 (2006).

[38] B. Chevalier, M.L. Kahn, J.-L. Bobet, M. Pasturel, J. Etourneau, *J. Phys., Condens. Matter* **14**, L365 (2002).

[39] S.K. Malik, D. Kundaliya, A. Sathyamoorthy, K. Shashikada, P. Raj, V.V. Krishnamurthy, *J. Appl. Phys.* **93**, 7834 (2003).